Outage Constrained Transmission Design for IRS-aided Communications with Imperfect Cascaded Channels

Gui Zhou[1], Cunhua Pan[1], Hong Ren[1], Kezhi Wang[2], and Arumugam Nallanathan[1]
[1]School of Electronic Engineering and Computer Science at Queen Mary University of London, U.K.
[2]Department of Computer and Information Sciences, Northumbria University, U.K.
e-mail: {g.zhou, c.pan, h.ren, a.nallanathan}@qmul.ac.uk, kezhi.wang@northumbria.ac.uk.

***Abstract*—Intelligent reflection surface (IRS) has recently been recognized as a promising technique to enhance the performance of wireless systems due to its ability of reconfiguring the signal propagation environment. However, the perfect channel state information (CSI) is challenging to obtain at the base station (BS) due to the lack of radio frequency (RF) chains at the IRS. Since most of the existing channel estimation methods were developed to acquire the cascaded BS-IRS-user channels, this paper is the first work to study the robust beamforming based on the imperfect cascaded BS-IRS-user channels at the transmitter (CBIUT). Specifically, the transmit power minimization problems are formulated subject to the rate outage probability constraints under the statistical CSI error model, respectively. After approximating the rate outage probability constraints by using the Bernstein-type inequality, the reformulated problems can be efficiently solved. Numerical results show that the negative impact of the CBIUT error on the system performance is greater than that of the direct CSI error.**

***Index Terms*—Intelligent reflecting surface (IRS), large intelligent surface (LIS), robust design, imperfect channel state information (CSI), cascaded BS-IRS-user channels at the transmitter (CBIUT).**

I. Introduction

Intelligent reflecting surface (IRS), which is also known as reconfigurable intelligent surface (RIS) or large intelligent surface (LIS), has emerged as a promising technique to enhance the spectral and energy efficiency of the wireless networks [1]–[3], thanks to its artificial planar passive radio array structure which is cost-effective and energy-efficient. More explicitly, each passive element on the IRS is capable of reconfiguring the channels between the BS and users constructively or destructively by imposing an independent phase shift to the incident signal. The existing literature on IRS-aided wireless communications has demonstrated that IRS is an enabler for enhancing the spectral and energy efficiency through jointly optimizing the active beamforming at the BS and the passive beamforming at the IRS [4]–[10]. However, the algorithms developed in the above contributions were based on the assumption of perfect channel state information at the transmitter (CSIT).

Unfortunately, it is challenging to estimate the channels for the IRS-aided wireless systems, since IRS is passive and can neither send nor receive pilot symbols. In general, there are two main approaches to estimate the IRS-related channels. The first approach is to directly estimate the IRS-related channels, i.e., estimate BS-IRS channel and IRS-user channels separately [11]. The another more popular method is to estimate the cascaded BS-IRS-user channels which are the product of the BS-IRS channel and the IRS-user channels [12]–[15]. The cascaded channel state information (CSI) is sufficient for the joint active and passive beamforming design [8]–[10]. Due to the inevitable channel estimation error, [16] and [17] proposed worst-case robust beamforming designs under the bounded channel error model. However, the robust design algorithms in [16] and [17] rely on the first channel estimation approach, where the BS-IRS channels and IRS-user channels should be independently estimated. This is difficult to achieve since several active elements should be installed at the IRS [11].

Against the above background, this is the first work to study the robust transmission design based on the imperfect cascaded BS-IRS-user channels at the transmitter (CBIUT), which is more practical than the previous works in which only imperfect IRS-user channels were considered. The contributions of this work are summarized as follows: 1) We aim to minimize the transmit power subject to unit-modulus constraints and the rate outage probability constraints. Here, the rate outage probability constraints represent the probability that the achievable rate of each user being below its minimum rate requirment needs to be less than a predetermined probability. 2) To address this problem, the Bernstein-Type Inequality is firstly adopted to approximate the rate outage probability. Then, under the alternate optimization (AO) framework, the precoder and the reflection beamforming is optimized by using the semidefinite relaxation (SDR) in an iterative manner. 3) We demonstrate through numerical results that the level of the CBIUT error plays an important role in the IRS-aided systems. Specifically, when the CBIUT error is small, the total transmit power decreases with the number of the reflection elements due to the increased beamforming gain. However, when the CBIUT error is large, the transmit power increases with the number of the reflection elements due to the increased channel estimation error.

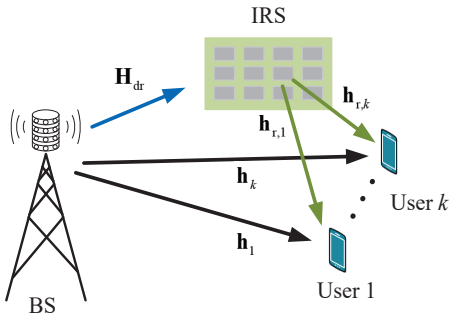

Fig. 1: An IRS-aided multi-user communication system.

II. System Model

A. Signal Transmission Model

As shown in Fig. 1, we consider an IRS-aided MISO broadcast (BC) communication system, which consists of one multi-antenna BS, K single-antenna users and one IRS. It is assumed that the BS equipped with N active antennas transmits K Gaussian data symbols denoted by $\mathbf{s} = [s_1, \cdots, s_K]^{\rm T} \in \mathbb{C}^{K\times 1}$ to all the users, where $\mathbb{E}[\mathbf{s}\mathbf{s}^{\rm H}] = \mathbf{I}$. IRS with M passive phase shifters is deployed to enhance the system performance. Therefore, by defining the set of users as $\mathcal{K} = \{1, 2, ..., K\}$, the received baseband signal of users is given by

$$y_k = (\mathbf{h}_k^{\rm H} + \mathbf{h}_{{\rm r},k}^{\rm H}\mathbf{E}\mathbf{H}_{\rm dr})\mathbf{F}\mathbf{s} + n_k, \forall k \in \mathcal{K}. \tag{1}$$

Here, $\mathbf{F} = [\mathbf{f}_1, \cdots, \mathbf{f}_K] \in \mathbb{C}^{N\times K}$ is the precoder matrix, in which $\mathbf{f}_k$ is the precoding vector associated with user k. Then, the transmit power at the BS is $\mathbb{E}\{{\rm Tr}\left[\mathbf{F}\mathbf{s}\mathbf{s}^{\rm H}\mathbf{F}^{\rm H}\right]\} = ||\mathbf{F}||_F^2$. n_k is the additive white Gaussian noise (AWGN) at user k, with zero mean and noise variance σ_k^2, i.e., $n_k \sim \mathcal{CN}(0, \sigma_k^2)$. The reflection beamforming of the IRS is a diagonal matrix $\mathbf{E} = {\rm diag}(e_1, \cdots, e_M) \in \mathbb{C}^{M\times M}$, of which has unit modulus, i.e., $|e_m|^2 = 1$. It is assumed that the phase shifts of the IRS are calculated by the BS and then fed back to the IRS controller through dedicated feedback channels [4], [5]. In addition, the channel vectors spanning from the BS to user k and from the IRS to user k are denoted by $\mathbf{h}_k \in \mathbb{C}^{N\times 1}$ and $\mathbf{h}_{{\rm r},k} \in \mathbb{C}^{M\times 1}$, respectively. The channel matrix between the BS and the IRS is represented by $\mathbf{H}_{\rm dr} \in \mathbb{C}^{M\times N}$.

Denote by $\mathbf{G}_k = {\rm diag}(\mathbf{h}_{{\rm r},k}^{\rm H})\mathbf{H}_{\rm dr}$ the cascaded channel from the BS to user k via the IRS, by $\mathbf{e} = [e_1, \cdots, e_M]^{\rm T} \in \mathbb{C}^{M\times 1}$ the vector containing diagonal elements of matrix $\mathbf{E}$, and by $\beta_k = ||(\mathbf{h}_k^{\rm H} + \mathbf{e}^{\rm H}\mathbf{G}_k)\mathbf{F}_{-k}||_2^2 + \sigma_k^2$ the interference-plus-noises (INs) power of user k, where $\mathbf{F}_{-k} = [\mathbf{f}_1, \cdots, \mathbf{f}_{k-1}, \mathbf{f}_{k+1}, \cdots, \mathbf{f}_K]$. Then, the achievable data rate (bit/s/Hz) at user k is given by

$$\mathcal{R}_k(\mathbf{F}, \mathbf{e}) = \log_2\left(1 + \frac{1}{\beta_k}\left|\left(\mathbf{h}_k^{\rm H} + \mathbf{e}^{\rm H}\mathbf{G}_k\right)\mathbf{f}_k\right|^2\right). \tag{2}$$

B. Two Scenarios and CSI Error Models

In the IRS-aided communication system, there are two types of channels: the direct channel $\mathbf{h}_k$ and the cascaded BS-IRS-user channel $\mathbf{G}_k$. Next, we first introduce two scenarios of the channel uncertainties and then CSI error model.

1) Scenario 1: Partial Channel Uncertainty (PCU)

In IRS-aided communications, the CBIUT is much more challenging to obtain than the direct channel state information at the transmitter (DCSIT) due to the passive features of the IRS. Hence, in this scenario, we assume perfect DCSIT and imperfect CBIUT which is represented as

$$\mathbf{G}_k = \widehat{\mathbf{G}}_k + \triangle\mathbf{G}_k, \forall k \in \mathcal{K}, \tag{3}$$

where $\widehat{\mathbf{G}}_k$ is the estimated cascaded CSI known at the BS, $\triangle\mathbf{G}_k$ is the unknown CBIUT error.

2) Scenario 2: Full Channel Uncertainty (FCU)

In complex electromagnetic environment, the accurate DCSIT is also challenging to obtain. In this scenario, we assume both the DCSIT and the CBIUT are imperfect. In addition to the CBIUT error model in (3), the direct channel is given by

$$\mathbf{h}_k = \widehat{\mathbf{h}}_k + \triangle\mathbf{h}_k, \forall k \in \mathcal{K}, \tag{4}$$

where $\widehat{\mathbf{h}}_k$ is the estimated DCSIT known at the BS and $\triangle\mathbf{h}_k$ is the unknown DCSIT error.

In general, the channel estimation error follows the Gaussian distribution [13]. Hence, the statistical CSI error model is considered in this work. Specifically, each CSI error vector is assumed to follow the circularly symmetric complex Gaussian (CSCG) distribution, i.e.,

$${\rm vec}(\triangle\mathbf{G}_k) \sim \mathcal{CN}(\mathbf{0}, \mathbf{\Sigma}_{{\rm g},k}), \mathbf{\Sigma}_{{\rm g},k} \succeq \mathbf{0}, \forall k \in \mathcal{K}, \tag{5a}$$

$$\triangle\mathbf{h}_k \sim \mathcal{CN}(\mathbf{0}, \mathbf{\Sigma}_{{\rm h},k}), \mathbf{\Sigma}_{{\rm h},k} \succeq \mathbf{0}, \forall k \in \mathcal{K}, \tag{5b}$$

where $\mathbf{\Sigma}_{{\rm g},k} \in \mathbb{C}^{MN\times MN}$ and $\mathbf{\Sigma}_{{\rm h},k} \in \mathbb{C}^{N\times N}$ are positive semidefinite error covariance matrices. In this case, the CSI imperfection is caused by the channel estimation error. For example, in the time division duplex (TDD) setting, noise and limited training will cause the uplink channel estimation error. The conventional MMSE method is generally adopted to estimate the cascaded channel, and thus the channel estimation generally follows the CSCG distribution.

III. Outage Constrained Beamforming Design

In this section, the outage constrained robust beamforming design is considered under the statistical CSI error model. Specifically, by defining the maximum data rate outage probabilities $\rho_1, ..., \rho_K \in (0, 1]$, the transmit power minimization problem is formulated as

$$\min_{\mathbf{F},\mathbf{e}} \ ||\mathbf{F}||_F^2 \tag{6a}$$

$$\text{s.t. } \Pr\{\mathcal{R}_k(\mathbf{F}, \mathbf{e}) \geq R_k\} \geq 1 - \rho_k, \forall k \in \mathcal{K} \tag{6b}$$

$$|e_m|^2 = 1, 1 \leq m \leq M. \tag{6c}$$

The rate outage constraints (6b) guarantee that the probability of each user that can successfully decode its message at a data rate of R_k is no less than $1 - \rho_k$.

Problem (6) is computationally intractable due to the fact that the constraints (6b) have no simple closed-form expressions [18]. In order to solve Problem (6), a safe approximation based on Bernstein-type inequality is given in the following lemma.

Lemma 1 *(Bernstein-Type Inequality [18]) Assume* $f(\mathbf{x}) = \mathbf{x}^{\mathrm{H}}\mathbf{U}\mathbf{x} + 2\mathrm{Re}\{\mathbf{u}^{\mathrm{H}}\mathbf{x}\} + u$*, where* $\mathbf{U} \in \mathbb{H}^{n\times n}$*,* $\mathbf{u} \in \mathbb{C}^{n\times 1}$*,* $u \in \mathbb{R}$ *and* $\mathbf{x} \in \mathbb{C}^{n\times 1} \sim \mathcal{CN}(\mathbf{0}, \mathbf{I})$*. Then for any* $\rho \in [0, 1]$*, the following approximation holds:*

$$\Pr\{\mathbf{x}^{\mathrm{H}}\mathbf{U}\mathbf{x} + 2\mathrm{Re}\{\mathbf{u}^{\mathrm{H}}\mathbf{x}\} + u \geq 0\} \geq 1 - \rho \tag{7a}$$

$$\Rightarrow \mathrm{Tr}\{\mathbf{U}\} - \sqrt{2\ln(1/\rho)}x + \ln(\rho)\lambda^{+}_{\max}(-\mathbf{U}) + u \geq 0 \tag{7b}$$

$$\Rightarrow \begin{cases} \mathrm{Tr}\{\mathbf{U}\} - \sqrt{2\ln(1/\rho)}x + \ln(\rho)y + u \geq 0 \\ \sqrt{||\mathbf{U}||_F^2 + 2||\mathbf{u}||^2} \leq x \\ y\mathbf{I} + \mathbf{U} \succeq \mathbf{0}, y \geq 0, \end{cases} \tag{7c}$$

where $\lambda^{+}_{\max}(-\mathbf{U}) = \max(\lambda_{\max}(-\mathbf{U}), 0)$*.* x *and* y *are slack variables.*

A. Scenario 1: Partial Channel Uncertainty

Before the derivations, the rate outage probability of user k in (6b) is rewritten as

$$\begin{aligned}&\Pr\left\{\log_2\left(1 + \frac{\left|\left(\mathbf{h}_k^{\mathrm{H}} + \mathbf{e}^{\mathrm{H}}\mathbf{G}_k\right)\mathbf{f}_k\right|^2}{\left\|\left(\mathbf{h}_k^{\mathrm{H}} + \mathbf{e}^{\mathrm{H}}\mathbf{G}_k\right)\mathbf{F}_{-k}\right\|_2^2 + \sigma_k^2}\right) \geq R_k\right\} \\ &= \Pr\left\{\left(\mathbf{h}_k^{\mathrm{H}} + \mathbf{e}^{\mathrm{H}}\mathbf{G}_k\right)\mathbf{\Phi}_k\left(\mathbf{h}_k + \mathbf{G}_k^{\mathrm{H}}\mathbf{e}\right) - \sigma_k^2 \geq 0\right\},\end{aligned} \tag{8}$$

where $\mathbf{\Phi}_k = \mathbf{f}_k\mathbf{f}_k^{\mathrm{H}}/(2^{R_k} - 1) - \mathbf{F}_{-k}\mathbf{F}_{-k}^{\mathrm{H}}$.

For the convenience of derivations, we assume that $\mathbf{\Sigma}_{\mathrm{g},k} = \varepsilon_{\mathrm{g},k}^2\mathbf{I}$, then the RCSIT error in (5) can be rewritten as $\mathrm{vec}(\triangle\mathbf{G}_k) = \varepsilon_{\mathrm{g},k}\mathbf{i}_{\mathrm{g},k}$ where $\mathbf{i}_{\mathrm{g},k} \sim \mathcal{CN}(\mathbf{0}, \mathbf{I})$. Defining $\mathbf{E} = \mathbf{e}\mathbf{e}^{\mathrm{H}}$, the rate outage probability (8) is reformulated in (9) at the top of the next page. Therefore, the rate outage constraints (6b) are given as

$$\begin{aligned}&\Pr\left\{\mathbf{i}_{\mathrm{g},k}^{\mathrm{H}}\mathbf{U}_k\mathbf{i}_{\mathrm{g},k} + 2\mathrm{Re}\{\mathbf{u}_k^{\mathrm{H}}\mathbf{i}_{\mathrm{g},k}\} + u_k \geq 0\right\} \\ &\quad\geq 1 - \rho_k, \forall k \in \mathcal{K},\end{aligned} \tag{10}$$

where

$$\mathbf{U}_k = \varepsilon_{\mathrm{g},k}^2(\mathbf{\Phi}_k^{\mathrm{T}} \otimes \mathbf{E}), \tag{11a}$$

$$\mathbf{u}_k = \varepsilon_{\mathrm{g},k}\mathrm{vec}((\mathbf{e}\mathbf{h}_k^{\mathrm{H}} + \mathbf{E}\widehat{\mathbf{G}}_k)\mathbf{\Phi}_k^{\mathrm{H}}), \tag{11b}$$

$$u_k = (\mathbf{h}_k^{\mathrm{H}} + \mathbf{e}^{\mathrm{H}}\widehat{\mathbf{G}}_k)\mathbf{\Phi}_k(\mathbf{h}_k + \widehat{\mathbf{G}}_k^{\mathrm{H}}\mathbf{e}) - \sigma_k^2. \tag{11c}$$

Applying Lemma 1 and introducing auxiliary variables $\mathbf{x} = [x_1, ..., x_K]^{\mathrm{T}}$ and $\mathbf{y} = [y_1, ..., y_K]^{\mathrm{T}}$, constraint of user k in (10) is transformed into the deterministic form as

$$\mathrm{Tr}\{\mathbf{U}_k\} - \sqrt{2\ln(1/\rho_k)}x_k + \ln(\rho_k)y_k + u_k \geq 0, \tag{12a}$$

$$\sqrt{||\mathbf{U}_k||_F^2 + 2||\mathbf{u}_k||^2} \leq x_k, \tag{12b}$$

$$y_k\mathbf{I} + \mathbf{U}_k \succeq \mathbf{0}, y_k \geq 0. \tag{12c}$$

(12) can be further simplified by some mathematical transformations as follows

$$\mathrm{Tr}\{\mathbf{U}_k\} = \varepsilon_{\mathrm{g},k}^2\mathrm{Tr}\left\{\mathbf{\Phi}_k^{\mathrm{T}} \otimes \mathbf{E}\right\} = \varepsilon_{\mathrm{g},k}^2\mathrm{Tr}\{\mathbf{\Phi}_k\}\mathrm{Tr}\{\mathbf{E}\}$$

$$= \varepsilon_{\mathrm{g},k}^2 M\mathrm{Tr}\{\mathbf{\Phi}_k\}, \tag{13a}$$

$$\begin{aligned}||\mathbf{U}_k||_F^2 &= \varepsilon_{\mathrm{g},k}^4||(\mathbf{\Phi}_k^{\mathrm{T}} \otimes \mathbf{E})||_F^2 = \varepsilon_{\mathrm{g},k}^4||\mathbf{\Phi}_k||_F^2||\mathbf{E}||_F^2 \\ &= \varepsilon_{\mathrm{g},k}^4 M^2||\mathbf{\Phi}_k||_F^2,\end{aligned} \tag{13b}$$

$$\begin{aligned}||\mathbf{u}_k||^2 &= \varepsilon_{\mathrm{g},k}^2||\mathrm{vec}((\mathbf{e}\mathbf{h}_k^{\mathrm{H}} + \mathbf{E}\widehat{\mathbf{G}}_k)\mathbf{\Phi}_k^{\mathrm{H}})||^2 \\ &= \varepsilon_{\mathrm{g},k}^2 M||\left(\mathbf{h}_k^{\mathrm{H}} + \mathbf{e}^{\mathrm{H}}\widehat{\mathbf{G}}_k\right)\mathbf{\Phi}_k||_2^2,\end{aligned} \tag{13c}$$

$$\begin{aligned}\lambda(\mathbf{U}_k) &= \lambda(\varepsilon_{\mathrm{g},k}^2(\mathbf{\Phi}_k^{\mathrm{T}} \otimes \mathbf{E})) = \varepsilon_{\mathrm{g},k}^2\lambda(\mathbf{\Phi}_k^{\mathrm{T}} \otimes \mathbf{E}) \\ &= \varepsilon_{\mathrm{g},k}^2\lambda(\mathbf{\Phi}_k)\lambda(\mathbf{E}) = \varepsilon_{\mathrm{g},k}^2 M\lambda(\mathbf{\Phi}_k).\end{aligned} \tag{13d}$$

Operation $\lambda(\mathbf{X})$ means the eigenvalues of $\mathbf{X}$. (13a) and (13b) are from [P76 in [19]], (13d) is from [P421 in [19]].

Therefore, according to Lemma 1 and equation (13), the approximation problem of Problem (6) can be given as

$$\min_{\mathbf{F},\mathbf{e},\mathbf{x},\mathbf{y}} \ ||\mathbf{F}||_F^2 \tag{14a}$$

$$\text{s.t. } \varepsilon_{\mathrm{g},k}^2 M\mathrm{Tr}\{\mathbf{\Phi}_k\} - \sqrt{2\ln(1/\rho_k)}x_k - \ln(1/\rho_k)y_k + u_k \geq 0, \forall k \in \mathcal{K} \tag{14b}$$

$$\left\| \begin{array}{c} \varepsilon_{\mathrm{g},k}^2 M\mathrm{vec}(\mathbf{\Phi}_k) \\ \sqrt{2M}\varepsilon_{\mathrm{g},k}\mathbf{\Phi}_k\left(\mathbf{h}_k + \widehat{\mathbf{G}}_k^{\mathrm{H}}\mathbf{e}\right) \end{array} \right\| \leq x_k, \forall k \in \mathcal{K} \tag{14c}$$

$$y_k\mathbf{I} + \varepsilon_{\mathrm{g},k}^2 M\mathbf{\Phi}_k \succeq \mathbf{0}, y_k \geq 0, \forall k \in \mathcal{K} \tag{14d}$$

$$|e_m|^2 = 1, \forall m \in \mathcal{M}. \tag{14e}$$

Problem (14) is still difficult to solve due to the non-convex constraints (14e) and (14c) as well as coupled variables $\mathbf{F}$ and $\mathbf{e}$. We use AO method to update $\mathbf{F}$ and $\mathbf{e}$ in an iterative manner.

For fixed $\mathbf{e}$, let $\mathbf{\Phi}_k = \mathbf{\Gamma}_k/(2^{R_k} - 1) - \sum_{i=1,i\neq k}^{K}\mathbf{\Gamma}_i$ where $\mathbf{\Gamma}_k = \mathbf{f}_k\mathbf{f}_k^{\mathrm{H}}$, Problem (14) corresponding to $\mathbf{F}$ is given as

$$\min_{\mathbf{\Gamma},\mathbf{x},\mathbf{y}} \ \sum_{k=1}^{K}\mathrm{Tr}\{\mathbf{\Gamma}_k\} \tag{15a}$$

$$\text{s.t. } \varepsilon_{\mathrm{g},k}^2 M\mathrm{Tr}\{\mathbf{\Phi}_k\} - \sqrt{2\ln(1/\rho_k)}x_k - \ln(1/\rho_k)y_k + u_k \geq 0, \forall k \in \mathcal{K} \tag{15b}$$

$$\left\| \begin{array}{c} \varepsilon_{\mathrm{g},k}^2 M\mathrm{vec}(\mathbf{\Phi}_k) \\ \sqrt{2M}\varepsilon_{\mathrm{g},k}\mathbf{\Phi}_k\left(\mathbf{h}_k + \widehat{\mathbf{G}}_k^{\mathrm{H}}\mathbf{e}\right) \end{array} \right\| \leq x_k, \forall k \in \mathcal{K} \tag{15c}$$

$$y_k\mathbf{I} + \varepsilon_{\mathrm{g},k}^2 M\mathbf{\Phi}_k \succeq \mathbf{0}, y_k \geq 0, \forall k \in \mathcal{K} \tag{15d}$$

$$\mathbf{\Gamma}_k \succeq \mathbf{0}, \forall k \in \mathcal{K} \tag{15e}$$

$$\mathrm{rank}(\mathbf{\Gamma}_k) = 1, \forall k \in \mathcal{K}, \tag{15f}$$

where $\mathbf{\Gamma} = [\mathbf{\Gamma}_1, ..., \mathbf{\Gamma}_K]$. Problem (15) can be solved by adopting the SDR technique, i.e., removing $\mathrm{rank}(\mathbf{\Gamma}_k) = 1, \forall k \in \mathcal{K}$ from the problem formulation, the resulting convex SDP problem is then efficiently solved by the CVX tools. Numerical results show that, the optimal $\mathbf{\Gamma}_k^{\star}$ is usually of rank one. The optimal $\mathbf{f}_k$ can be obtained from $\mathbf{\Gamma}_k^{\star}$ by using eigenvalue decomposition.

Then, for given $\mathbf{F}$, the subproblem of $\mathbf{e}$ is a feasibility-check problem. According to [16], [20] and in order to improve the converged solution in the optimization of $\mathbf{e}$, we introduce the slack variables $\boldsymbol{\alpha} = [\alpha_1, ..., \alpha_K]^{\mathrm{T}} \geq 0$ to the rate outage

$$
\begin{aligned}
&\Pr\left\{\left(\mathbf{h}_k^{\mathrm{H}}+\mathbf{e}^{\mathrm{H}}(\widehat{\mathbf{G}}_k+\triangle\mathbf{G}_k)\right)\mathbf{\Phi}_k\left(\mathbf{h}_k+(\widehat{\mathbf{G}}_k+\triangle\mathbf{G}_k)^{\mathrm{H}}\mathbf{e}\right)-\sigma_k^2\geq 0\right\}\\
&=\Pr\Big\{\mathrm{vec}^{\mathrm{H}}(\triangle\mathbf{G}_k)(\mathbf{\Phi}_k^{\mathrm{T}}\otimes\mathbf{E})\mathrm{vec}(\triangle\mathbf{G}_k)+2\mathrm{Re}\{\mathrm{vec}^{\mathrm{H}}((\mathbf{e}\mathbf{h}_k^{\mathrm{H}}+\mathbf{E}\widehat{\mathbf{G}}_k)\mathbf{\Phi}_k)\mathrm{vec}(\triangle\mathbf{G}_k)\}\\
&\quad+(\mathbf{h}_k^{\mathrm{H}}+\mathbf{e}^{\mathrm{H}}\widehat{\mathbf{G}}_k)\mathbf{\Phi}_k(\mathbf{h}_k+\widehat{\mathbf{G}}_k^{\mathrm{H}}\mathbf{e})-\sigma_k^2\geq 0\Big\}\\
&=\Pr\left\{\varepsilon_{\mathrm{g},k}^2\mathbf{i}_{\mathrm{g},k}^{\mathrm{H}}(\mathbf{\Phi}_k^{\mathrm{T}}\otimes\mathbf{E})\mathbf{i}_{\mathrm{g},k}+2\mathrm{Re}\{\varepsilon_{\mathrm{g},k}\mathrm{vec}^{\mathrm{H}}((\mathbf{e}\mathbf{h}_k^{\mathrm{H}}+\mathbf{E}\widehat{\mathbf{G}}_k)\mathbf{\Phi}_k)\mathbf{i}_{\mathrm{g},k}\}+(\mathbf{h}_k^{\mathrm{H}}+\mathbf{e}^{\mathrm{H}}\widehat{\mathbf{G}}_k)\mathbf{\Phi}_k(\mathbf{h}_k+\widehat{\mathbf{G}}_k^{\mathrm{H}}\mathbf{e})-\sigma_k^2\geq 0\right\}. \quad (9)
\end{aligned}
$$

probability in (8) and have

$$\Pr\left\{\left(\mathbf{h}_k^{\mathrm{H}}+\mathbf{e}^{\mathrm{H}}\mathbf{G}_k\right)\mathbf{\Phi}_k\left(\mathbf{h}_k+\mathbf{G}_k^{\mathrm{H}}\mathbf{e}\right)-\sigma_k^2-\alpha_k\geq 0\right\}.$$

Then, (11c) is also modified as follows

$$
\begin{aligned}
u_k^{\mathbf{e}}&=(\mathbf{h}_k^{\mathrm{H}}+\mathbf{e}^{\mathrm{H}}\widehat{\mathbf{G}}_k)\mathbf{\Phi}_k(\mathbf{h}_k+\widehat{\mathbf{G}}_k^{\mathrm{H}}\mathbf{e})-\sigma_k^2-\alpha_k.\\
&=\mathrm{Tr}\left\{\mathbf{C}_k\widehat{\mathbf{E}}\right\}+\mathbf{h}_k^{\mathrm{H}}\mathbf{\Phi}_k\mathbf{h}_k-\sigma_k^2-\alpha_k \quad (16)
\end{aligned}
$$

where

$$\mathbf{C}_k=\begin{bmatrix}\widehat{\mathbf{G}}_k\mathbf{\Phi}_k\widehat{\mathbf{G}}_k^{\mathrm{H}} & \widehat{\mathbf{G}}_k\mathbf{\Phi}_k\mathbf{h}_k\\ \mathbf{h}_k^{\mathrm{H}}\mathbf{\Phi}_k\widehat{\mathbf{G}}_k^{\mathrm{H}} & 0\end{bmatrix},\widehat{\mathbf{E}}=\widehat{\mathbf{e}}\widehat{\mathbf{e}}^{\mathrm{H}},\widehat{\mathbf{e}}=\begin{bmatrix}\mathbf{e}\\ 1\end{bmatrix}.$$

With variable $\widehat{\mathbf{E}}$, (14c) is rewritten as

$$
\begin{aligned}
&\varepsilon_{\mathrm{g},k}^4M^2||\mathbf{\Phi}_k||_F^2+2\varepsilon_{\mathrm{g},k}^2M\left(\mathrm{Tr}\left\{\mathbf{R}_k\widehat{\mathbf{E}}\right\}+\mathbf{h}_k^{\mathrm{H}}\mathbf{\Phi}_k^{\mathrm{H}}\mathbf{\Phi}_k\mathbf{h}_k\right)\\
&\leq 2\mathrm{Re}\{x_k^{(n)}x_k\}-x_k^{(n),2},\forall k\in\mathcal{K} \quad (17)
\end{aligned}
$$

where $x_k^{(n)}$ is the optimal solution of the n-th iteration.

In addition, constraints (14d) are independent of $\mathbf{e}$ and transformed from $\lambda_{\max}^{+}(-\mathbf{U})$ in Lemma 1, we then can have $y_k=\max(\lambda_{\max}(-\varepsilon_{\mathrm{g},k}^2M\mathbf{\Phi}_k),0),\forall k\in\mathcal{K}$.

Finally, the subproblem of (14) corresponding to $\mathbf{e}$ is formulated as

$$
\begin{aligned}
\max_{\widehat{\mathbf{E}},\boldsymbol{\alpha},\mathbf{x}}\ &\sum_{k=1}^{K}\alpha_k && (18a)\\
\text{s.t. }&\varepsilon_{\mathrm{g},k}^2M\mathrm{Tr}\{\mathbf{\Phi}_k\}-\sqrt{2\ln(1/\rho_k)}x_k-\ln(1/\rho_k)y_k\\
&+u_k^{\mathbf{e}}\geq 0,\forall k\in\mathcal{K} && (18b)\\
&(17),\boldsymbol{\alpha}\geq 0 && (18c)\\
&\widehat{\mathbf{E}}\succeq\mathbf{0},\mathrm{rank}(\widehat{\mathbf{E}})=1,[\widehat{\mathbf{E}}]_{k,k}=1,\forall k\in\mathcal{K}. && (18d)
\end{aligned}
$$

After adopting the SDR technique, the relaxed Problem (18), which is a convex SDP problem, is solved by the CVX tools. The optimal $\mathbf{e}$ can be obtained from the optimal $\widehat{\mathbf{E}}^{\star}$ by using Gaussian randomization techniques.

B. Scenario 2: Full Channel Uncertainty

In this subsection, we extend the outage constrained robust beamforming design from the partial channel uncertainty to the case where all the channels are imperfect at the BS. By considering the full statistical CSI error in (5), (8) is then formulated as

$$
\begin{aligned}
&\Pr\Big\{\left(\widehat{\mathbf{h}}_k^{\mathrm{H}}+\mathbf{e}^{\mathrm{H}}\widehat{\mathbf{G}}_k\right)\mathbf{\Phi}_k\left(\widehat{\mathbf{h}}_k+\widehat{\mathbf{G}}_k^{\mathrm{H}}\mathbf{e}\right)\\
&+2\mathrm{Re}\left\{\left(\widehat{\mathbf{h}}_k^{\mathrm{H}}+\mathbf{e}^{\mathrm{H}}\widehat{\mathbf{G}}_k\right)\mathbf{\Phi}_k\left(\triangle\mathbf{h}_k+\triangle\mathbf{G}_k^{\mathrm{H}}\mathbf{e}\right)\right\}-\sigma_k^2\\
&+\left(\triangle\mathbf{h}_k^{\mathrm{H}}+\mathbf{e}^{\mathrm{H}}\triangle\mathbf{G}_k\right)\mathbf{\Phi}_k\left(\triangle\mathbf{h}_k+\triangle\mathbf{G}_k^{\mathrm{H}}\mathbf{e}\right)\geq 0\Big\}. \quad (19)
\end{aligned}
$$

Assuming that $\mathbf{\Sigma}_{\mathrm{h},k}=\varepsilon_{\mathrm{h},k}^2\mathbf{I}$, then the DCSIT can be expressed as $\triangle\mathbf{h}_k=\varepsilon_{\mathrm{h},k}\mathbf{i}_{\mathrm{h},k}$ where $\mathbf{i}_{\mathrm{h},k}\sim\mathcal{CN}(\mathbf{0},\mathbf{I})$. The second term inside (19) is rewritten as

$$
\begin{aligned}
&2\mathrm{Re}\Big\{(\widehat{\mathbf{h}}_k^{\mathrm{H}}+\mathbf{e}^{\mathrm{H}}\widehat{\mathbf{G}}_k)\mathbf{\Phi}_k\triangle\mathbf{h}_k\\
&\quad+\mathrm{vec}^{\mathrm{T}}(\mathbf{e}(\widehat{\mathbf{h}}_k^{\mathrm{H}}+\mathbf{e}^{\mathrm{H}}\widehat{\mathbf{G}}_k)\mathbf{\Phi}_k)\mathrm{vec}(\triangle\mathbf{G}_k^{*})\Big\}\\
&=2\mathrm{Re}\Big\{\varepsilon_{\mathrm{h},k}(\widehat{\mathbf{h}}_k^{\mathrm{H}}+\mathbf{e}^{\mathrm{H}}\widehat{\mathbf{G}}_k)\mathbf{\Phi}_k\mathbf{i}_{\mathrm{h},k}\\
&\quad+\varepsilon_{\mathrm{g},k}\mathrm{vec}^{\mathrm{T}}(\mathbf{e}(\widehat{\mathbf{h}}_k^{\mathrm{H}}+\mathbf{e}^{\mathrm{H}}\widehat{\mathbf{G}}_k)\mathbf{\Phi}_k)\mathbf{i}_{\mathrm{g},k}^{*}\Big\}\\
&=2\mathrm{Re}\left\{\widetilde{\mathbf{u}}_k^{\mathrm{H}}\widetilde{\mathbf{i}}_k\right\},
\end{aligned}
$$

where $\widetilde{\mathbf{i}}_k=\begin{bmatrix}\mathbf{i}_{\mathrm{h},k}^{\mathrm{H}} & \mathbf{i}_{\mathrm{g},k}^{\mathrm{T}}\end{bmatrix}^{\mathrm{H}}$ and

$$\widetilde{\mathbf{u}}_k=\begin{bmatrix}\varepsilon_{\mathrm{h},k}\mathbf{\Phi}_k(\widehat{\mathbf{h}}_k+\widehat{\mathbf{G}}_k^{\mathrm{H}}\mathbf{e})\\ \varepsilon_{\mathrm{g},k}\mathrm{vec}^{*}(\mathbf{e}(\widehat{\mathbf{h}}_k^{\mathrm{H}}+\mathbf{e}^{\mathrm{H}}\widehat{\mathbf{G}}_k)\mathbf{\Phi}_k)\end{bmatrix}.$$

The forth term on the left hand side of (19) is rewritten as

$$
\begin{aligned}
&\triangle\mathbf{h}_k^{\mathrm{H}}\mathbf{\Phi}_k\triangle\mathbf{h}_k+2\mathrm{Re}\left\{\mathbf{e}^{\mathrm{H}}\triangle\mathbf{G}_k\mathbf{\Phi}_k\triangle\mathbf{h}_k\right\}\\
&\quad+\mathbf{e}^{\mathrm{H}}\triangle\mathbf{G}_k\mathbf{\Phi}_k\triangle\mathbf{G}_k^{\mathrm{H}}\mathbf{e}\\
&=\varepsilon_{\mathrm{h},k}^2\mathbf{i}_{\mathrm{h},k}^{\mathrm{H}}\mathbf{\Phi}_k\mathbf{i}_{\mathrm{h},k}+2\mathrm{Re}\left\{\triangle\mathbf{h}_k^{\mathrm{H}}(\mathbf{\Phi}_k\otimes\mathbf{e}^{\mathrm{T}})\mathrm{vec}(\triangle\mathbf{G}_k^{*})\right\}\\
&\quad+\mathrm{vec}^{\mathrm{T}}(\triangle\mathbf{G}_k)(\mathbf{\Phi}_k\otimes\mathbf{E}^{\mathrm{T}})\mathrm{vec}(\triangle\mathbf{G}_k^{*})\\
&=\varepsilon_{\mathrm{h},k}^2\mathbf{i}_{\mathrm{h},k}^{\mathrm{H}}\mathbf{\Phi}_k\mathbf{i}_{\mathrm{h},k}+2\mathrm{Re}\left\{\varepsilon_{\mathrm{h},k}\varepsilon_{\mathrm{g},k}\mathbf{i}_{\mathrm{h},k}^{\mathrm{H}}(\mathbf{\Phi}_k\otimes\mathbf{e}^{\mathrm{T}})\mathbf{i}_{\mathrm{g},k}^{*}\right\}\\
&\quad+\varepsilon_{\mathrm{g},k}^2\mathbf{i}_{\mathrm{g},k}^{\mathrm{T}}(\mathbf{\Phi}_k\otimes\mathbf{E}^{\mathrm{T}})\mathbf{i}_{\mathrm{g},k}^{*}\\
&=\widetilde{\mathbf{i}}_k^{\mathrm{H}}\widetilde{\mathbf{U}}_k\widetilde{\mathbf{i}}_k,
\end{aligned}
$$

where

$$\widetilde{\mathbf{U}}_k=\begin{bmatrix}\mathbf{\Sigma}_{\mathrm{h},k}^{1/2}\mathbf{\Phi}_k\mathbf{\Sigma}_{\mathrm{h},k}^{1/2} & \varepsilon_{\mathrm{h},k}\varepsilon_{\mathrm{g},k}(\mathbf{\Phi}_k\otimes\mathbf{e}^{\mathrm{T}})\\ \varepsilon_{\mathrm{h},k}\varepsilon_{\mathrm{g},k}(\mathbf{\Phi}_k\otimes\mathbf{e}^{*}) & \varepsilon_{\mathrm{g},k}^2(\mathbf{\Phi}_k\otimes\mathbf{E}^{\mathrm{T}})\end{bmatrix}.$$

Denote $\widetilde{u}_k=(\widehat{\mathbf{h}}_k^{\mathrm{H}}+\mathbf{e}^{\mathrm{H}}\widehat{\mathbf{G}}_k)\mathbf{\Phi}_k(\widehat{\mathbf{h}}_k+\widehat{\mathbf{G}}_k^{\mathrm{H}}\mathbf{e})-\sigma_k^2$, the rate outage constraint (19) is then equivalent to

$$\Pr\left\{\widetilde{\mathbf{i}}_k^{\mathrm{H}}\widetilde{\mathbf{U}}_k\widetilde{\mathbf{i}}_k+2\mathrm{Re}\left\{\widetilde{\mathbf{u}}_k^{\mathrm{H}}\widetilde{\mathbf{i}}_k\right\}+\widetilde{u}_k\geq 0\right\}\geq 1-\rho_k. \quad (20)$$

Combining Lemma 1 and new auxiliary variables $\widetilde{\mathbf{x}}=[\widetilde{x}_1,...,\widetilde{x}_K]^{\mathrm{T}}$ and $\widetilde{\mathbf{y}}=[\widetilde{y}_1,...,\widetilde{y}_K]^{\mathrm{T}}$, the approximation of the data rate outage constraint of user k in (20) is given by

$$
\begin{aligned}
&\mathrm{Tr}\left\{\widetilde{\mathbf{U}}_k\right\}-\sqrt{2\ln(1/\rho_k)}\widetilde{x}_k+\ln(\rho_k)\widetilde{y}_k+\widetilde{u}_k\geq 0, \quad (21a)\\
&\sqrt{||\widetilde{\mathbf{U}}_k||_F^2+2||\widetilde{\mathbf{u}}_k||^2}\leq\widetilde{x}_k, \quad (21b)
\end{aligned}
$$

TABLE I: System parameters

Path loss exponent of BS-user link	$\alpha_{\mathrm{BU}} = 4$
Path loss exponent of BS-IRS link	$\alpha_{\mathrm{BI}} = 2.2$
Path loss exponent of IRS-user link	$\alpha_{\mathrm{IU}} = 2$
Noise power	$\{\sigma_k^2\}_{k=1}^K = -80$ dBm
Convergence tolerance	10^{-4}
Maximun outage probabilities	$\{\rho_k^2\}_{k=1}^K = 0.05$

$$\widetilde{y}_k\mathbf{I} + \widetilde{\mathbf{U}}_k \succeq \mathbf{0}, \widetilde{y}_k \geq 0. \tag{21c}$$

We simplify some terms in (21) as follows:

$$\begin{aligned}\mathrm{Tr}\left\{\widetilde{\mathbf{U}}_k\right\} &= \mathrm{Tr}\left\{\left[\begin{array}{c}\varepsilon_{\mathrm{h},k}\boldsymbol{\Phi}_k^{1/2}\\ \varepsilon_{\mathrm{g},k}(\boldsymbol{\Phi}_k^{1/2}\otimes\mathbf{e}^*)\end{array}\right]\right.\\ &\quad\left.\bullet\left[\begin{array}{cc}\varepsilon_{\mathrm{h},k}\boldsymbol{\Phi}_k^{1/2} & \varepsilon_{\mathrm{g},k}(\boldsymbol{\Phi}_k^{1/2}\otimes\mathbf{e}^{\mathrm{T}})\end{array}\right]\right\}\\ &= (\varepsilon_{\mathrm{h},k}^2 + \varepsilon_{\mathrm{g},k}^2 M)\mathrm{Tr}\left\{\boldsymbol{\Phi}_k\right\}, \end{aligned}\tag{22a}$$

$$||\widetilde{\mathbf{U}}_k||_F^2 = (\varepsilon_{\mathrm{h},k}^2 + \varepsilon_{\mathrm{g},k}^2 M)^2||\boldsymbol{\Phi}_k||_F^2, \tag{22b}$$

$$||\widetilde{\mathbf{u}}_k||^2 = (\varepsilon_{\mathrm{h},k}^2 + \varepsilon_{\mathrm{g},k}^2 M)||(\widehat{\mathbf{h}}_k^{\mathrm{H}} + \mathbf{e}^{\mathrm{H}}\widehat{\mathbf{G}}_k)\boldsymbol{\Phi}_k||_2^2, \tag{22c}$$

$$\widetilde{y}_k\mathbf{I} + \widetilde{\mathbf{U}}_k \succeq \mathbf{0} \Longrightarrow \widetilde{y}_k\mathbf{I} + (\varepsilon_{\mathrm{h},k}^2 + \varepsilon_{\mathrm{g},k}^2 M)\boldsymbol{\Phi}_k \succeq \mathbf{0}. \tag{22d}$$

The derivations of (22) are similar to (13).

Based on the above results, Problem (6) with imperfect DCSIT and imperfect CBIUT is given by

$$\min_{\mathbf{F},\mathbf{e},\widetilde{\mathbf{x}},\widetilde{\mathbf{y}}} \ ||\mathbf{F}||_F^2 \tag{23a}$$

$$\begin{aligned}\text{s.t. } &(\varepsilon_{\mathrm{h},k}^2 + \varepsilon_{\mathrm{g},k}^2 M)\mathrm{Tr}\left\{\boldsymbol{\Phi}_k\right\} - \sqrt{2\ln(1/\rho_k)}x_k\\ &- \ln(1/\rho_k)y_k + \widetilde{u}_k \geq 0, \forall k \in \mathcal{K}\end{aligned}\tag{23b}$$

$$\left\|\begin{array}{c}(\varepsilon_{\mathrm{h},k}^2 + \varepsilon_{\mathrm{g},k}^2 M)\mathrm{vec}(\boldsymbol{\Phi}_k)\\ \sqrt{2(\varepsilon_{\mathrm{h},k}^2 + \varepsilon_{\mathrm{g},k}^2 M)}\boldsymbol{\Phi}_k\left(\widehat{\mathbf{h}}_k + \widehat{\mathbf{G}}_k^{\mathrm{H}}\mathbf{e}\right)\end{array}\right\| \leq \widetilde{x}_k, \tag{23c}$$

$$\forall k \in \mathcal{K} \tag{23d}$$

$$\widetilde{y}_k\mathbf{I} + (\varepsilon_{\mathrm{h},k}^2 + \varepsilon_{\mathrm{g},k}^2 M)\boldsymbol{\Phi}_k \succeq \mathbf{0}, \widetilde{y}_k \geq 0, \forall k \in \mathcal{K} \tag{23e}$$

$$|e_m|^2 = 1, \forall m \in \mathcal{M}. \tag{23f}$$

Comparing Problem (23) with Problem (14), we find that the former can be obtained from the latter by replacing $\varepsilon_{\mathrm{g},k}^2 M$ with $\varepsilon_{\mathrm{h},k}^2 + \varepsilon_{\mathrm{g},k}^2 M$ and $\mathbf{h}_k$ wtih $\widehat{\mathbf{h}}_k$. Therefore, Problem (23) can be solved by using the same techniques as those used to solve Problem (14). In addition, when M is large, the impact of imperfect CBIUT dominates the performance of the system, which will be illustrated in the numerical results later. Thus, it is significant to investigate the robust beamforming in IRS-aided system in which there are a large number of reflection elements with high channel estimation error.

IV. Numerical Results and Discussions

In this section, we provide numerical results to evaluate the performance of our proposed algorithms. We assume that the BS is located at (0 m, 0 m) and the IRS is placed at (50 m, 10 m). K users are randomly and uniformly distributed in a circle centered at (70 m, 0 m) with radius of 5 m. The channel models, i.e., $\{\mathbf{h}_k, \mathbf{G}_k\}_{\forall k\in\mathcal{K}}$, are assumed to include large-scale fading and small-scale fading. The large-scale fading model is expressed as $\mathrm{PL} = -30 - 10\alpha\log_{10}(d)$ dB, where α is the path loss exponent and d is the link distance in meters. The small-scale fading in $\{\mathbf{h}_k, \mathbf{G}_k\}_{\forall k\in\mathcal{K}}$ is assumed to be Rayleigh fading distribution. For the statistical CSI error model, the variance of $\mathrm{vec}(\triangle\mathbf{G}_k)$ and $\triangle\mathbf{h}_k$ are defined as $\varepsilon_{\mathrm{g},k}^2 = \delta_{\mathrm{g}}^2||\mathrm{vec}(\widehat{\mathbf{G}}_k)||_2^2$ and $\varepsilon_{\mathrm{h},k}^2 = \delta_{\mathrm{h}}^2||\widehat{\mathbf{h}}_k||_2^2$, respectively. $\delta_{\mathrm{g}} \in [0, 1)$ and $\delta_{\mathrm{h}} \in [0, 1)$ measure the relative amount of CSI uncertainties. In addition, the target rates of all users are assumed to be the same, i.e., $R_1 = ... = R_K = R$ and the fixed simulation settings are given in Table I.

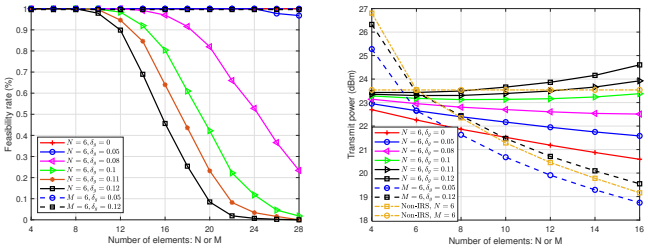

(a) Feasibility rate (b) Transmit power

Fig. 2: Feasibility rate and transmit power versus the number of antenna elements under the PCU scenario, when $K = 2$.

Fig. 2 shows the feasibility rate and the minimum transmit power versus N or M when only the CBIUT is imperfect, i.e., $\delta_{\mathrm{h}} = 0$. We assume there are $K = 2$ users with $R = 2$ bit/s/Hz. The feasibility rate is defined as the ratio of the number of feasible channel realizations to the total number of channel realizations, where the feasible channel realization means that there exists a feasible solution to the outage constrained problem in (6) for this channel realization. An interesting phenomenon can be observed from Fig. 6 (a). When fixing N, the feasibility rate decreases rapidly with the number of phase shifters at a high level of channel uncertainty ($\delta_{\mathrm{g}} \geq 0.08$). By contrast, when fixing M the feasibility rate keeps stable for different numbers of antennas even at a high level of channel uncertainty.

Based on the observations of Fig. 2(a), we further examine the minimum transmit power consumption of different channel uncertainty levels in Fig. 2(b) with a benchmark scheme without IRS. Fig. 2(b) is generated based on the channel realizations for which the feasible solutions can be obtained at $N = 16$ or $M = 16$.

We first study the case with fixed $N = 6$. In Fig. 2(b), the case with $\delta_{\mathrm{g}} = 0$ can be regarded as the perfect CBIUT case, and its minimum transmit power decreases with M. This trend is consistent with that of Fig. 4 in [20]. The minimum transmit power under small values of δ_{g}, e.g., $\delta_{\mathrm{g}} = \{0.05, 0.08\}$, also decrease with the number of the reflection elements, and are higher than that of the perfect CBIUT case. The reason is

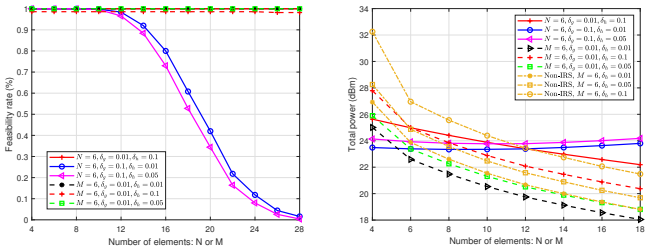

(a) Feasibility rate (b) Transmit power

Fig. 3: Feasibility rate and transmit power versus the number of antenna elements under the FCU scenario, when $K = 2$.

that the BS needs to consume more power to compensate for the rate loss caused by the CBIUT error. However, when δ_{g} increases to 0.1 or larger, transmit power consumption starts to increase with the number of reflection elements. The reason is that increasing the number of reflection elements can not only reduce the transmit power due to its increased beamforming gain, but also increase the channel estimation error that more transmit power is required to compensate for the channel errors. Therefore, when the CBIUT error is small, the benefits brought by the increase of M, outweighs its drawbacks, and vice versa. As a result, the number of IRS reflection elements should be carefully chosen, and the accuracy of the CBIUT estimation is crucial to reap the benefits offered by the IRS.

On the other hand, for the case with fixed number of reflection elements, the transmit power consumption values decrease with the number of antennas at the BS even when the CBIUT error is high as $\delta_{\mathrm{g}} = 0.12$. The reason is that when the number of antennas is large, more degrees of freedom can be exploited to optimize the active beamforming vector at the BS to compensate for the channel estimation error. Finally, compared with the system without IRS, the IRS may lose its performance gain advantage under high CBIUT error.

Fig. 3 shows the feasibility rate and the minimum transmit power versus M or N when both the DCSIT and the CBIUT are imperfect. The simulation parameters are the same as those in Fig. 2. Fig. 3(a) shows that when δ_{g} is low, the feasibility rates achieved by various cases are always high. In addition, from Fig. 3(b), we find that the increase of the number of antennas at the BS is effective in reducing the transmit power consumption, which is not affected by the DCSIT error δ_{h} (see curves $M = 6, \delta_{\mathrm{g}} = 0.01, \delta_{\mathrm{h}} = \{0.01, 0.05, 0.1\}$).

V. Conclusions

In this work, we have investigated robust beamforming designs under imperfect CBIUT for the IRS-aided MU-MISO system. Our aim is to minimize the transmit power subject to the rate outage probability constraints under the statistical CSI error model. The CSI uncertainties under the statistical CSI error model have been tackled by using the Bernstein-Type Inequality. The reformulated problems have then been efficiently solved under the AO framework. It is shown that the number of elements on the IRS may have a negative impact on system performance when the CBIUT error is large. This conclusion provides an engineering insight for the careful selection of the size of the IRS.

References

[1] E. Basar, M. Di Renzo, J. de Rosny *et al.*, "Wireless communications through reconfigurable intelligent surfaces," *IEEE Access*, vol. 7, pp. 116 753–116 773, Aug. 2019.

[2] K. Ntontin, M. Di Renzo, J. Song *et al.*, "Reconfigurable intelligent surfaces vs. relaying: Differences, similarities, and performance comparison," *IEEE Open J. Commun. Soc.*, vol. 1, pp. 798–807, 2020.

[3] X. Yuan, Y.-J. Zhang, Y. Shi, W. Yan, and H. Liu, "Reconfigurable-intelligent-surface empowered 6G wireless communications: Challenges and opportunities," 2019. [Online]. Available: https://arxiv.org/abs/2001.00364

[4] C. Pan, H. Ren, K. Wang, M. Elkashlan, A. Nallanathan, J. Wang, and L. Hanzo, "Intelligent reflecting surface aided MIMO broadcasting for simultaneous wireless information and power transfer," *IEEE J. Sel. Areas Commun.*, vol. 38, no. 8, pp. 1719–1734, Jun. 2020.

[5] C. Pan, H. Ren, K. Wang, W. Xu, M. Elkashlan, A. Nallanathan, and L. Hanzo, "Multicell MIMO communications relying on intelligent reflecting surface," *IEEE Trans. Wireless Commun.*, vol. 19, no. 8, pp. 5218–5233, May 2020.

[6] T. Bai, C. Pan, Y. Deng, M. Elkashlan, and A. Nallanathan, "Latency minimization for intelligent reflecting surface aided mobile edge computing," *IEEE J. Sel. Areas Commun., early access*, 2020.

[7] H. Han, J. Zhao, D. Niyato *et al.*, "Intelligent reflecting surface aided network: Power control for physical-layer broadcasting," *ICC 2020*.

[8] G. Zhou, C. Pan, H. Ren, K. Wang, and A. Nallanathan, "Intelligent Reflecting Surface Aided Multigroup Multicast MISO Communication Systems," *IEEE Trans. Signal Process.*, vol. 68, pp. 3236–3251, Apr. 2020.

[9] H. Shen, W. Xu, S. Gong, Z. He, and C. Zhao, "Secrecy rate maximization for intelligent reflecting surface assisted multi-antenna communications," *IEEE Commun. Lett.*, vol. 23, no. 9, pp. 1488–1492, Jun 2019.

[10] S. Zhang and R. Zhang, "Capacity characterization for intelligent reflecting surface aided MIMO communication," *IEEE J. Sel. Areas Commun.*, vol. 38, no. 8, pp. 1823–1838, Jun 2020.

[11] A. Taha, M. Alrabeiah, and A. Alkhateeb, "Enabling large intelligent surfaces with compressive sensing and deep learning," 2019. [Online]. Available: https://arxiv.org/abs/1904.10136

[12] Z. Zhou, N. Ge, Z. Wang, and L. Hanzo, "Joint transmit precoding and reconfigurable intelligent surface phase adjustment: A decomposition-aided channel estimation approach," 2019. [Online]. Available: https://www.researchgate.net/publication/337824343

[13] Z. Wang, L. Liu, and S. Cui, "Channel estimation for intelligent reflecting surface assisted multiuser communications: Framework, algorithms, and analysis," *IEEE Trans. Wireless Commun., early access*, 2020.

[14] P. Wang, J. Fang, H. Duan, and H. Li, "Compressed channel estimation and joint beamforming for intelligent reflecting surface-assisted millimeter wave systems," *IEEE Signal Processing Lett.*, vol. 27, pp. 905–909, May 2020.

[15] J. Chen, Y.-C. Liang, H. V. Cheng, and W. Yu, "Channel estimation for reconfigurable intelligent surface aided multi-user MIMO systems," 2019. [Online]. Available: https://arxiv.org/abs/1912.03619

[16] G. Zhou, C. Pan, H. Ren, K. Wang, M. Di Renzo, and A. Nallanathan, "Robust beamforming design for intelligent reflecting surface aided MISO communication systems," *IEEE Commun. Lett., early access*, 2020.

[17] X. Yu, D. Xu, Y. Sun, D. W. K. Ng, and R. Schober, "Robust and secure wireless communications via intelligent reflecting surfaces," *IEEE J. Sel. Areas Commun., early access*, 2020.

[18] K. Wang, A. M. So, T. Chang, W. Ma, and C. Chi, "Outage constrained robust transmit optimization for multiuser miso downlinks: Tractable approximations by conic optimization," *IEEE Trans. Signal Process.*, vol. 62, no. 21, pp. 5690–5705, Nov. 2014.

[19] X.-D. Zhang, *Matrix analysis and applications*. Cambridge Univ. Press, 2017.

[20] Q. Wu and R. Zhang, "Intelligent reflecting surface enhanced wireless network via joint active and passive beamforming," *IEEE Trans. Wireless Commun.*, vol. 18, no. 11, pp. 5394–5409, Nov. 2019.